# Approximate Minimum Bit-Error Rate Equalization for Pulse-Amplitude and Quadrature-Amplitude Modulation

Chen-Chu Yeh and John R. Barry

School of Electrical and Computer Engineering
Georgia Institute of Technology, Atlanta, Georgia 30332-0250

***Abstract*** — We propose the *approximate minimum-bit-error-rate* (*AMBER*) algorithm for adapting the coefficients of a linear equalizer with pulse-amplitude and quadrature-amplitude modulation. While less complex than the least-mean-square algorithm, AMBER very nearly minimizes error probability in white Gaussian noise, and can significantly outperform the minimum-mean-squared-error equalizer when the number of equalizer coefficients is small relative to the severity of the intersymbol interference.

## I. Introduction

The most popular design strategy for finite-tap linear equalization with memoryless detection is the minimum mean-squared-error (MMSE) strategy. However, a better strategy is to choose the equalizer coefficients to minimize error probability directly [1–3]. Prior adaptive equalization algorithms for minimizing error probability were restricted to binary modulation [3][4], and some were high in complexity [3]. In this paper we propose the *approximate minimum-bit-error-rate* (*AMBER*) algorithm, a generalization of the binary adaptation algorithm of [4] to multilevel pulse-amplitude modulation (PAM) and higher-order quadrature amplitude modulation (QAM).

Although the least-mean square (LMS) algorithm for minimizing MSE has low complexity, several variations of LMS have been devised to reduce complexity even further, such as the sign LMS [6] and dual-sign LMS [7]. We will show that the AMBER algorithm is remarkably similar in form to these LMS-based algorithms, despite the fact that it originates from a minimum-BER criterion rather than a desire to reduce complexity. In particular, the AMBER algorithm can be viewed as the sign LMS algorithm modified to update only when a decision error is made.

This paper is organized as follows. In Sect. II, we present models for the channel and equalizer. In Sect. III, we propose the approximate minimum-BER algorithm for PAM and QAM. In Sect. IV, we present numerical results showing that the proposed algorithm very nearly minimizes error probability, outperforming the MMSE equalizer by 14 dB in one example.

## II. Problem Statement

We consider the linear discrete-time system depicted in Fig. 1, where the channel input symbols $x_k$ are drawn independently and uniformly from the $L$-ary PAM alphabet $\{\pm1, \pm3, \ldots, \pm(L-1)\}$, $h_k$ is the FIR channel impulse response nonzero for $k = 0 \ldots M$ only, and $n_k$ is white Gaussian noise with power spectral density $\sigma^2$. The equalizer output is $y_k = \boldsymbol{c}^T\boldsymbol{r}_k$, where $\boldsymbol{c}$ is a vector of $N$ equalizer coefficients and $\boldsymbol{r}_k = \mathbf{H}\boldsymbol{x}_k + \boldsymbol{n}_k$ is a vector of channel outputs, where $\mathbf{H}$ is an $N \times (M + N)$ matrix with $H_{ij} = h_{j-i}$, $\boldsymbol{x}_k = [x_k \ \ldots \ x_{k-M-N+1}]^T$ is a vector of channel inputs, and $\boldsymbol{n}_k$ is the noise vector. The decision $\hat{x}_{k-D}$ about symbol $x_{k-D}$ is determined by quantizing the equalizer output $y_k$, where $D$ accounts for the delay of both the channel and the equalizer.

Let $\boldsymbol{f}^T = \boldsymbol{c}^T\mathbf{H} = [f_0 \ \ldots \ f_{M+N-1}]$ denote the overall impulse response. The noiseless equalizer output is then:

$$\boldsymbol{f}^T\boldsymbol{x}_k = f_D x_{k-D} + \sum\nolimits_{i \neq D} f_i x_{k-i}. \tag{1}$$

The first term $f_D x_{k-D}$ represents the desired signal, whereas the second term represents interference. Because the probability distribution of the interference term is symmetric, the optimal decision thresholds after any equalizer are $\{0, \pm 2f_D, \ldots, \pm(L-2)f_D\}$.

Let $\tilde{\boldsymbol{x}}$ denote a random vector with distribution $p(\tilde{\boldsymbol{x}}) = p(\boldsymbol{x}_k \mid x_{k-D} = 1)$, *i.e.*, $\tilde{\boldsymbol{x}}$ is uniformly distributed over the set of $L^{M+N-1}$ $L$-ary $\boldsymbol{x}_k$ vectors for which $x_{k-D} = 1$. It can then be shown that, with optimal decision thresholds, the probability of symbol error after any equalizer is:

$$P_e(\boldsymbol{c}) = \frac{2L-2}{L}\,\mathrm{E}\left[Q\left(\frac{\boldsymbol{c}^T\mathbf{H}\tilde{\boldsymbol{x}}}{\|\boldsymbol{c}\|\sigma}\right)\right], \tag{2}$$

where $Q$ is the Gaussian error function. Observe that the error probability depends on $\boldsymbol{c}$ only through the ratio $\boldsymbol{c}/\|\boldsymbol{c}\|$.

In the sections that follow we develop an adaptive algorithm for finding $\boldsymbol{c}$ so as to approximately minimize the error probability (2). We will restrict consideration to *equalizable* channels for which there exists an equalizer capable of opening the noiseless eye diagram; *i.e.*, there exists a $\boldsymbol{c}$ such that $\boldsymbol{c}^T\mathbf{H}\tilde{\boldsymbol{x}} > 0$ for all $L$-ary vectors $\tilde{\boldsymbol{x}}$ for which $x_{k-D} = 1$.

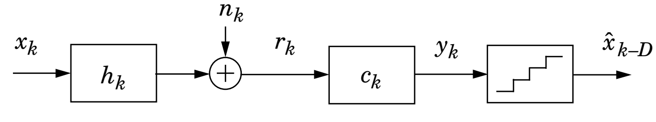


**Fig. 1.** System block diagram.

## III. Approximate Minimum-BER Equalization

By setting to zero the gradient of (2) with respect to the equalizer $\boldsymbol{c}$, we find that the $\boldsymbol{c}$ minimizing error probability must satisfy the fixed-point relationship $\boldsymbol{c} = ag(\boldsymbol{c})$ for some $a > 0$, where the vector function $g : \mathbb{R}^N \longrightarrow \mathbb{R}^N$ is defined by:

$$g(\boldsymbol{c}) \overset{\Delta}{=} \mathrm{E}\left[\frac{1}{2}\exp\left(\frac{-(\boldsymbol{c}^T\mathbf{H}\tilde{\boldsymbol{x}})^2}{2\|\boldsymbol{c}\|^2\sigma^2}\right)\mathbf{H}\tilde{\boldsymbol{x}}\right] \tag{3}$$

$$\approx \mathrm{E}\left[Q\left(\frac{\boldsymbol{c}^T\mathbf{H}\tilde{\boldsymbol{x}}}{\|\boldsymbol{c}\|\sigma}\right)\mathbf{H}\tilde{\boldsymbol{x}}\right] \overset{\Delta}{=} q(\boldsymbol{c}). \tag{4}$$

In (4) we define the function $q(\boldsymbol{c})$ that approximates $g(\boldsymbol{c})$ by replacing $0.5e^{-x^2/2}$ by $Q(x)$. It can be shown [5] that, although there may be numerous unit-norm solutions to the fixed-point equation $\boldsymbol{c} = ag(\boldsymbol{c})$ for $a > 0$, there is only *one* unit-norm solution to $\boldsymbol{c} = aq(\boldsymbol{c})$ for $a > 0$; call it $\boldsymbol{c}_{AMBER}$. And while this equalizer no longer minimizes BER exactly, the accuracy with which $Q(x)$ approximates $0.5e^{-x^2/2}$ for small $x$ suggests that $\boldsymbol{c}_{AMBER}$ closely approximates the minimum-BER equalizer. The simulation results of Sect. IV substantiate this claim.

Here we propose a numerical algorithm to recover $\boldsymbol{c}_{AMBER}$. In fact, it can be proven [5] that the following algorithm is guaranteed to converge to the direction of the unique unit-norm vector $\boldsymbol{c}_{AMBER}$ satisfying $\boldsymbol{c} = aq(\boldsymbol{c})$ for $a > 0$:

$$\boldsymbol{c}_{k+1} = \boldsymbol{c}_k + \mu q(\boldsymbol{c}_k), \tag{5}$$

where $\mu$ is a positive step size.

Let us introduce an error indicator function $I(x_{k-D}, y_k)$ to indicate the *presence* and *sign* of an error: $I = 0$ if no error occurs, $I = 1$ if an error occurs because $y_k$ is too negative, and $I = -1$ if an error occurs because $y_k$ is too positive. In other words:

$$I = \begin{cases} 1, & \text{if } y_k < (x_{k-D} - 1)f_D \text{ and } x_{k-D} \neq -L + 1, \\ -1, & \text{if } y_k > (x_{k-D} + 1)f_D \text{ and } x_{k-D} \neq L - 1, \\ 0, & \text{otherwise.} \end{cases} \tag{6}$$

**Lemma 1.** The ensemble average $\mathrm{E}[I\boldsymbol{r}_k]$ is as follows:

$$\mathrm{E}[I\boldsymbol{r}_k] = \frac{2L-2}{L}\{q(\boldsymbol{c}) - \varepsilon(\boldsymbol{c})\boldsymbol{c}\} \tag{7}$$

where $\varepsilon(\boldsymbol{c})$ is some positive constant.

Proof: The proof of Lemma 1 is in Appendix I.

We can use the indicator function of (6) to approximate the deterministic update equation of (5):

$$\begin{aligned} \boldsymbol{c}_{k+1} &= \boldsymbol{c}_k + \mu q(\boldsymbol{c}_k) \\ &= (1 + \mu\varepsilon(\boldsymbol{c}_k))\,\boldsymbol{c}_k + \mu\mathrm{E}[I\,\boldsymbol{r}_k] \\ &\approx \boldsymbol{c}_k + \mu\mathrm{E}[I\,\boldsymbol{r}_k] \end{aligned} \tag{8}$$

where the inequality in (8) is accurate when $\mu\varepsilon(\boldsymbol{c})$ is small. Removing the expectation in (8) leads to:

$$\boldsymbol{c}_{k+1} = \boldsymbol{c}_k + \mu\, I\,\boldsymbol{r}_k. \tag{9}$$

We refer to this stochastic update as the *approximate minimum-BER* (*AMBER*) algorithm. When $L = 2$, (9) reverts back to the binary algorithm proposed in [4]. We remark that (9) has the same form as the LMS algorithm, except that $I_{LMS} = x_{k-D} - y_k$. Observe that AMBER is less complex than LMS, because (9) does not require a floating-point multiplication. AMBER can be viewed as the sign LMS algorithm [6] modified to update only when a symbol decision error is made.

The indicator function $I$ in (9) requires knowledge of $f_D$, which changes with time as $\boldsymbol{c}$ is being updated. Let $\hat{f}_D(k)$ denote the estimate of $f_D$ at time $k$. For a given $x_{k-D}$, the equalizer output $y_k$ has mean $f_D x_{k-D}$, so that the ratio $y_k / x_{k-D}$ has mean $f_D$. We can track $f_D$ using a simple moving average:

$$\hat{f}_D(k+1) = (1-\lambda)\hat{f}_D(k) + \lambda\frac{y_k}{x_{k-D}}, \tag{10}$$

where $\lambda$ is a small positive step size. The detection thresholds are then $\{0, \pm 2\hat{f}_D(k), \ldots, \pm(L-2)\hat{f}_D(k)\}$.

Because the AMBER algorithm (9) updates only when an error occurs (*i.e.*, when $I \neq 0$), the convergence rate will be slow when the error rate is low. To increase convergence speed, we can modify AMBER so that the equalizer updates not only when an error is made, but also when an error is *almost* made, *i.e.*, when the distance between the equalizer output and the nearest decision threshold is less than some small positive constant $\tau$. Mathematically, the modified indicator function is $I_\tau = 1$ if $y_k < (x_{k-D} - 1) f_D + \tau$ and $x_{k-D} \neq -L + 1$, $I_\tau = -1$ if $y_k > (x_{k-D} + 1)f_D - \tau$ and $x_{k-D} \neq L - 1$, and $I_\tau = 0$ otherwise. When $\tau = 0$, the modified AMBER algorithm reverts to (9). Besides increasing the convergence rate of AMBER, a positive $\tau$ prevents $\|\boldsymbol{c}_k\|$ from possibly shrinking to zero.

**Lemma 2.** If $\tau > 0$ in (9), $\|\boldsymbol{c}_k\|$ does not shrink to zero.

Proof: The proof of Lemma 2 is in Appendix II.

Although a formal proof of global convergence for the AMBER algorithm with $\tau > 0$ is not available, simulation results suggest the following conjecture:

**Conjecture.** If the channel is equalizable, there exists a sufficiently small step size $\mu$ such that the modified AMBER algorithm globally converges to a unique vector.

Generalizing AMBER to $L^2$-QAM is straightforward, since the in-phase and quadratic components of a QAM system can be viewed as two parallel PAM systems. The complex form of AMBER is:

$$\boldsymbol{c}_{k+1} = \boldsymbol{c}_k + \mu\, I\boldsymbol{r}_k^*, \tag{11}$$

where $I = I(x_{k-D}^R, y_k^R) + jI(x_{k-D}^I, y_k^I)$ and where the superscripts $R$ and $I$ are used to denote real and imaginary parts, respectively.

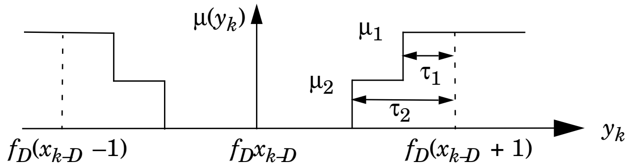


**Fig. 2.** Illustration of the 2-step AMBER algorithm.

The update frequency, and consequently the convergence speed, of the original AMBER is proportional to error probability. Although we have incorporated an update threshold $\tau$ to increase its convergence speed, a further increase in convergence speed may be realized by applying the dual-sign concept [7]. Instead of a single step size, we may use multiple step sizes such that updates occur more often. For example, a 2-step AMBER uses $\mu_1$ and $\mu_2$ for thresholds $\tau_1$ and $\tau_2$, as illustrated in Fig. 2.

## IV. Examples

We first consider a 4-PAM channel with severe ISI characterized by the transfer function $H(z) = 0.66 + z^{-1} - 0.66z^{-2}$. In Fig. 4 we plot symbol-error probability versus $\mathrm{SNR} = \sum_k |h_k|^2 / \sigma^2$ for three different five-tap linear equalizers: the MMSE equalizer, the exact minimum-error-probability (EMEP) equalizer, and the AMBER equalizer. In all cases the delay is $D = 3$, which is optimal for the MMSE equalizer. The coefficients of the MMSE and EMEP equalizers were calculated exactly, whereas the AMBER coefficients were obtained via the stochastic update (9), with $\mu = 0.0002$, $\tau = 0.05$, and $10^6$ training symbols. The symbol-error probability for all three equalizers was then evaluated using (2). Observe from Fig. 3 that the performance of AMBER is virtually indistinguishable from that of the EMEP equalizer, and that the AMBER equalizer outperforms the MMSE equalizer by over 14 dB at high SNR.

We now consider a 16QAM system with channel $H(z) = (0.5 + 0.3j) + (1.2 + 0.9j)z^{-1} - (0.6 + 0.4j)z^{-2}$. In Fig. 4 we plot symbol-error probability versus SNR for a four-tap linear MMSE equalizer and a four-tap linear AMBER equalizer. The MMSE delay $D = 3$ is used in both cases. The coefficients of the MMSE equalizer are exact, whereas the AMBER coefficients were obtained via (9) with $\mu = 0.0002$, $\tau = 0.05$, and $10^6$ training symbols. Both curves were obtained using Monte-Carlo techniques, averaged over $30 \times 10^6$ trials. Observe that AMBER outperforms MMSE by more than 6 dB.

In Fig. 5 and Fig. 6 we plot the first quadrant of the noiseless 16-QAM constellation diagrams after the AMBER and MMSE equalizers, respectively. The equalizers are scaled to have the same norm and therefore the same noise enhancement. Observe that the distance between the AMBER clouds is greater than the distance between the MMSE clouds. Thus, although the MSE of the AMBER equalizer is 0.5 dB higher than the MSE of the MMSE equalizer, the symbol-error probability is smaller by a factor of 17.

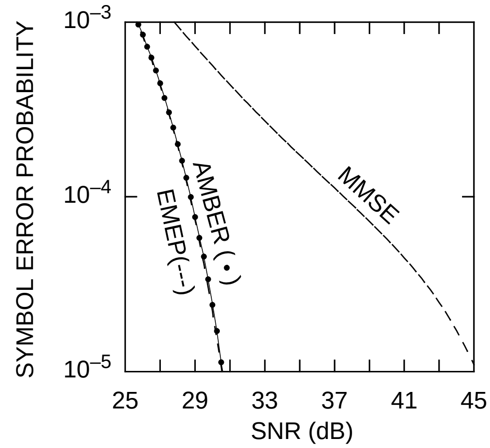


**Fig. 3.** Performance comparison for the 4-PAM example.

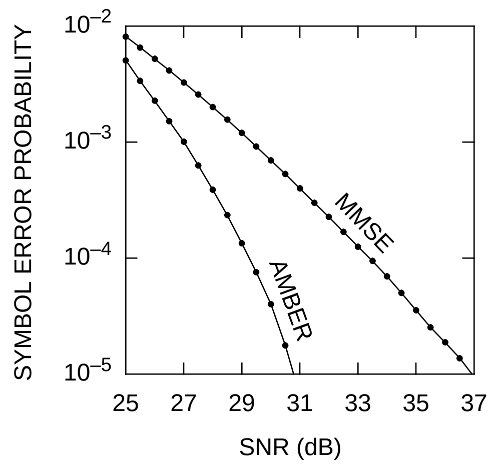


**Fig. 4.** Performance comparison for the 16-QAM example.

In Fig. 7, we compare the convergence rate of the LMS, AMBER, and 3-step AMBER algorithms for the channel $H(z) = 0.6 + z^{-1}$ with SNR = 30 dB. All equalizers have three taps and $D = 3$. A step size of $\mu = 0.0005$ is used for the LMS and AMBER algorithms, while a threshold of $\tau = 0.1$ is used for AMBER. For the 3-step AMBER, we use $\mu_1 = 0.002$, $\mu_2 = 0.001$, and $\mu_3 = 0.0005$ for $\tau_1 = 0$, $\tau_2 = 0.05$, and $\tau_3 = 0.1$. We see that the 3-step AMBER converges considerably faster than the AMBER algorithm.

## V. Conclusion

We have derived the approximate minimum-BER (AMBER) adaptive equalization algorithm for higher-order PAM and QAM. The AMBER algorithm very nearly minimizes error probability and is less complex than the LMS algorithm. We also proposed a variant of AMBER to increase convergence speed. When the number of equalizer coefficients is small relative to the severity of the channel ISI, the AMBER equalizer significantly outperforms the MMSE equalizer.

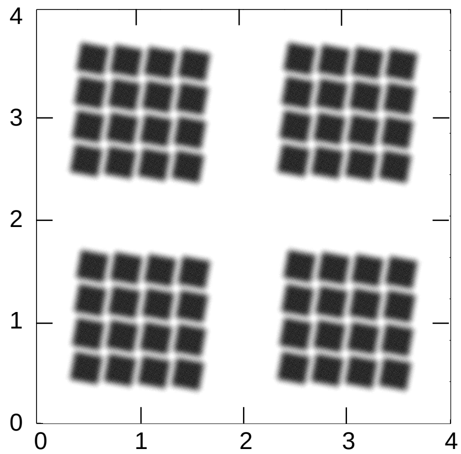

**Fig. 5.** Noiseless constellation (first quadrant only) after AMBER equalizer. (MSE = –5.4 dB, $P_e = 4.0 \times 10^{-5}$.)

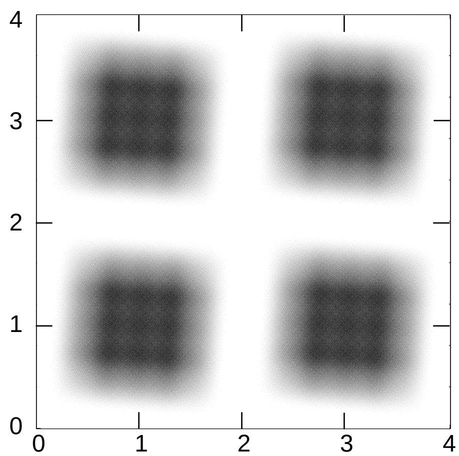

**Fig. 6.** Noiseless constellation (first quadrant only) after MMSE equalizer. (MSE = –5.9 dB, $P_e = 69.6 \times 10^{-5}$.)

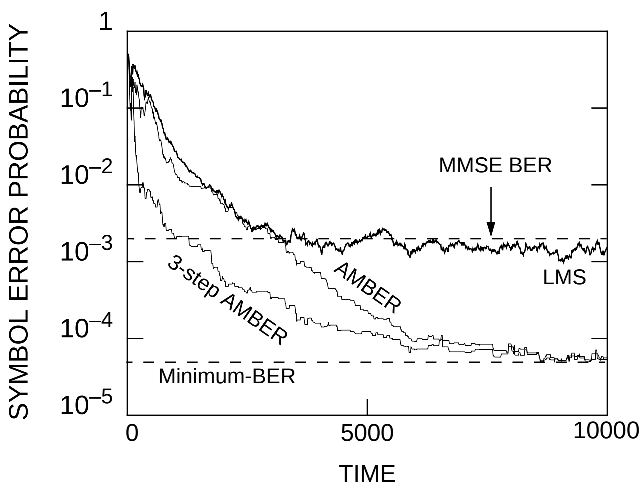


**Fig. 7.** Convergence of LMS, AMBER, and 3-step AMBER algorithms.

## Appendix I: Proof of Lemma 1

In this appendix we prove Lemma 1. Equivalently, because $\boldsymbol{r}_k = \mathbf{H}\boldsymbol{x}_k + \boldsymbol{n}_k$, we can decompose the equality of Lemma 1 into the following three equations:

$$\mathrm{E}[I x_{k-D}] = \frac{2L-2}{L}\mathrm{E}\left[Q\left(\frac{f_D + \boldsymbol{b}^T\boldsymbol{z}}{\|\boldsymbol{c}\|\sigma}\right)\right], \tag{12}$$

$$\mathrm{E}[I\boldsymbol{z}] = \frac{2L-2}{L}\mathrm{E}\left[Q\left(\frac{f_D + \boldsymbol{b}^T\boldsymbol{z}}{\|\boldsymbol{c}\|\sigma}\right)\boldsymbol{z}\right], \tag{13}$$

$$\mathrm{E}[I\boldsymbol{n}_k] = -\,\varepsilon(\boldsymbol{c})\boldsymbol{c}, \tag{14}$$

where we have defined $\boldsymbol{z} = [x_k, \ldots, x_{k-D+1}, x_{k-D-1}, \ldots, x_{k-M-N+1}]^T$ and $\boldsymbol{b} = [f_0, \ldots, f_{D-1}, f_{D+1}, \ldots, f_{M+N-1}]^T$ by discarding the $(D+1)$-st components of $\boldsymbol{x}_k$ and $\boldsymbol{f}$, respectively.

We first prove (12). Let "left", "right", and "inner" denote the events $x_{k-D} = -L+1$, $x_{k-D} = L-1$, and $x_{k-D} \in \{\pm 1, \pm 3, \ldots, \pm(L-3)\}$, respectively. (If $L = 2$, "inner" is the null event.) Then:

$$\begin{aligned}\mathrm{E}[I x_{k-D}] &= \mathrm{E}[I x_{k-D} \mid \text{left}]\mathrm{P}[\text{left}] + \mathrm{E}[I x_{k-D} \mid \text{right}]\mathrm{P}[\text{right}] + \\ &\qquad \mathrm{E}[I x_{k-D} \mid \text{inner}]\mathrm{P}[\text{inner}] \\ &= \frac{-L+1}{L}\mathrm{E}[I \mid \text{left}] + \frac{L-1}{L}\mathrm{E}[I \mid \text{right}] + \frac{L-2}{L}\mathrm{E}[I x_{k-D} \mid \text{inner}].\end{aligned} \tag{15}$$

But $I$ is independent of $x_{k-D}$ when $x_{k-D}$ is an inner point, so:

$$\mathrm{E}[I x_{k-D} \mid \text{inner}] = \mathrm{E}[I \mid \text{inner}]\mathrm{E}[x_{k-D} \mid \text{inner}] = \mathrm{E}[I \mid \text{inner}] \times 0 = 0. \tag{16}$$

Thus, (15) reduces to:

$$\begin{aligned}\mathrm{E}[I x_{k-D}] &= \frac{L-1}{L}\left\{-\mathrm{E}[\,I \mid \text{left}] + \mathrm{E}[I \mid \text{right}]\right\} \\ &= \frac{L-1}{L}\left\{-(1-\Pr[\,\boldsymbol{b}^T\boldsymbol{z} + \boldsymbol{c}^T\boldsymbol{n}_k > f_D]) + \Pr[\boldsymbol{b}^T\boldsymbol{z} + \boldsymbol{c}^T\boldsymbol{n}_k < -f_D]\right\} \\ &= \frac{L-1}{L}\left\{\mathrm{E}\left[Q\left(\frac{f_D - \boldsymbol{b}^T\boldsymbol{z}}{\|\boldsymbol{c}\|\sigma}\right)\right] + \mathrm{E}\left[Q\left(\frac{f_D + \boldsymbol{b}^T\boldsymbol{z}}{\|\boldsymbol{c}\|\sigma}\right)\right]\right\} \\ &= \frac{2L-2}{L}\mathrm{E}\left[Q\left(\frac{f_D + \boldsymbol{b}^T\boldsymbol{z}}{\|\boldsymbol{c}\|\sigma}\right)\right].\end{aligned} \tag{17}$$

The last equality follows because $\boldsymbol{z}$ and $-\boldsymbol{z}$ have the same distribution. This proves (12). Now we prove (13):

$$\mathrm{E}[I\boldsymbol{z}] = \frac{1}{L}\mathrm{E}[I\boldsymbol{z} \mid \text{left}] + \frac{1}{L}\mathrm{E}[I\boldsymbol{z} \mid \text{right}] + \frac{L-2}{L}\mathrm{E}[I\boldsymbol{z} \mid \text{inner}] \tag{18}$$

$$= \frac{1}{L}\mathrm{E}\left[\,\mathrm{E}[I \mid \boldsymbol{z}, \text{left}]\boldsymbol{z} + \mathrm{E}[I \mid \boldsymbol{z}, \text{right}]\boldsymbol{z} + (L-2)\mathrm{E}[\,I \mid \boldsymbol{z}, \text{inner}]\boldsymbol{z}\,\right] \tag{19}$$

$$\begin{aligned}&= \frac{1}{L}\mathrm{E}\left[-Q\left(\frac{f_D - \boldsymbol{b}^T\boldsymbol{z}}{\|\boldsymbol{c}\|\sigma}\right)\boldsymbol{z} + Q\left(\frac{f_D + \boldsymbol{b}^T\boldsymbol{z}}{\|\boldsymbol{c}\|\sigma}\right)\boldsymbol{z}\right. \\ &\qquad \left. + (L-2)\left\{Q\left(\frac{f_D + \boldsymbol{b}^T\boldsymbol{z}}{\|\boldsymbol{c}\|\sigma}\right) - Q\left(\frac{f_D - \boldsymbol{b}^T\boldsymbol{z}}{\|\boldsymbol{c}\|\sigma}\right)\right\}\boldsymbol{z}\right]\end{aligned} \tag{20}$$

$$= \frac{2L-2}{L} \mathrm{E}\left[ Q\left( \frac{f_D + \boldsymbol{b}^T \boldsymbol{z}}{\|\boldsymbol{c}\|\sigma} \right) \boldsymbol{z} \right]. \tag{21}$$

We now prove (14). First observe that:

$$\mathrm{E}[I\boldsymbol{n}_k] = \sum \mathrm{E}[I\boldsymbol{n}_k \mid I = 1, \boldsymbol{z} = \boldsymbol{z}^l]\,\mathrm{P}[I = 1, \boldsymbol{z} = \boldsymbol{z}^l] + \sum \mathrm{E}[I\boldsymbol{n}_k \mid I = -1, \boldsymbol{z} = \boldsymbol{z}^l]\,\mathrm{P}[I = -1, \boldsymbol{z} = \boldsymbol{z}^l] \tag{22}$$

where we omitted the summation term for $I = 0$ since it is zero and where both summations in (22) are summed over all $L^{M+N-1}$ possible $\boldsymbol{z}$ vectors. We will first derive $\mathrm{E}[I\boldsymbol{n}_k \mid I = 1, \boldsymbol{z} = \boldsymbol{z}^l]$:

$$\begin{aligned}\mathrm{E}[I\boldsymbol{n}_k \mid I = 1, \boldsymbol{z} = \boldsymbol{z}^l] &= \mathrm{E}[\boldsymbol{n}_k \mid \boldsymbol{c}^T\boldsymbol{n}_k < -f_D - \boldsymbol{b}^T\boldsymbol{z}^l, x_{k-D} \neq -L+1] \\ &= \mathrm{E}[\boldsymbol{n}_k \mid \boldsymbol{c}^T\boldsymbol{n}_k < -f_D - \boldsymbol{b}^T\boldsymbol{z}^l]. \end{aligned} \tag{23}$$

Now let $\mathbf{U}$ be any unitary matrix with first column equal to $\boldsymbol{c} / \| \boldsymbol{c} \|$. Then $\tilde{\boldsymbol{n}} = \mathbf{U}^T\boldsymbol{n}_k$ has the same statistics as $\boldsymbol{n}_k$, namely, the components of $\tilde{\boldsymbol{n}}$ are *i.i.d.* zero-mean Gaussian with variance $\sigma^2$. Furthermore, $\boldsymbol{c}^T\mathbf{U} = \| \boldsymbol{c} \| \boldsymbol{e}_1$, where $\boldsymbol{e}_1 = [1\ 0\ 0\ \dots\ 0]$, and $\boldsymbol{n}_k = \mathbf{U}\tilde{\boldsymbol{n}}$. Continuing with (23):

$$\mathrm{E}[\boldsymbol{n}_k \mid I = 1, \boldsymbol{z} = \boldsymbol{z}^l] = \mathrm{E}[\mathbf{U}\tilde{\boldsymbol{n}} \mid \boldsymbol{c}^T\mathbf{U}\tilde{\boldsymbol{n}} < -f_D - \boldsymbol{b}^T\boldsymbol{z}^l] \tag{24}$$

$$= \mathbf{U}\mathrm{E}[\tilde{\boldsymbol{n}} \mid \| \boldsymbol{c} \| \tilde{n}_1 < -f_D - \boldsymbol{b}^T\boldsymbol{z}^l] \tag{25}$$

$$= \mathbf{U}\mathrm{E}\left[ \tilde{\boldsymbol{n}} \mid \frac{-\tilde{n}_1}{\sigma} > \frac{f_D + \boldsymbol{b}^T\boldsymbol{z}^l}{\|\boldsymbol{c}\|\sigma} \right] \tag{26}$$

$$= -\sigma\mathbf{U}\mathrm{E}\left[ \frac{-\tilde{n}_1}{\sigma} \mid \frac{-\tilde{n}_1}{\sigma} > \frac{f_D + \boldsymbol{b}^T\boldsymbol{z}^l}{\|\boldsymbol{c}\|\sigma} \right] \boldsymbol{e}_1 \tag{27}$$

$$= -\sigma\, m\left( \frac{f_D + \boldsymbol{b}^T\boldsymbol{z}^l}{\|\boldsymbol{c}\|\sigma} \right) \boldsymbol{c} / \| \boldsymbol{c} \|, \tag{28}$$

where $m(\eta) = \frac{e^{-\eta^2/2}}{\sqrt{2\pi}Q(\eta)} \triangleq \mathrm{E}[X \mid X \geq \eta, X \sim \mathcal{N}(0,1)]$. We now derive the joint probability $\mathrm{P}[I = 1, \boldsymbol{z} = \boldsymbol{z}^l]$:

$$\begin{aligned}\mathrm{P}[I = 1, \boldsymbol{z} = \boldsymbol{z}^l] &= \mathrm{P}[I = 1 \mid \boldsymbol{z} = \boldsymbol{z}^l]\,\mathrm{P}[\boldsymbol{z} = \boldsymbol{z}^l] \\ &= \frac{L-1}{L} Q\left( \frac{f_D + \boldsymbol{b}^T\boldsymbol{z}^l}{\|\boldsymbol{c}\|\sigma} \right) \frac{1}{L^{M+N-1}}. \end{aligned} \tag{29}$$

Combining (28) and (29), the first summation in (22) becomes

$$\begin{aligned}&\sum \mathrm{E}[I\boldsymbol{n}_k \mid I = 1, \boldsymbol{z} = \boldsymbol{z}^l]\,\mathrm{P}[I = 1, \boldsymbol{z} = \boldsymbol{z}^l] \\ &= \sum_l \frac{-(L-1)\sigma}{L^{M+N}\sqrt{2\pi}} \exp\left( \frac{-(f_D + \boldsymbol{b}^T\boldsymbol{z}^l)^2}{2\|\boldsymbol{c}\|^2\sigma^2} \right) \frac{\boldsymbol{c}}{\|\boldsymbol{c}\|} \\ &= \frac{-(L-1)\sigma}{L\sqrt{2\pi}} \mathrm{E}\left[ \exp\left( \frac{-(f_D + \boldsymbol{b}^T\boldsymbol{z})^2}{2\|\boldsymbol{c}\|^2\sigma^2} \right) \right] \frac{\boldsymbol{c}}{\|\boldsymbol{c}\|}. \end{aligned} \tag{30}$$

It is not hard to show that the second summation in (22) turns out to be the same as (30). Hence, we conclude that

$$\mathrm{E}[I\boldsymbol{n}_k] = -\frac{2L-2}{L} \frac{\sigma}{\sqrt{2\pi}\|\boldsymbol{c}\|} \mathrm{E}\left[ \exp\left( \frac{-(f_D + \boldsymbol{b}^T\boldsymbol{z})^2}{2\|\boldsymbol{c}\|^2\sigma^2} \right) \right] \boldsymbol{c}. \tag{31}$$

## Appendix II: Proof of Lemma 2

Similar to the derivation in Appendix I, the ensemble average of (9) with $\tau > 0$ is derived to be:

$$\boldsymbol{c}_{k+1} = \{1 - \mu\varepsilon_\tau(\boldsymbol{c}_k)\}\boldsymbol{c}_k + \mu q_\tau(\boldsymbol{c}_k), \tag{32}$$

where

$$\varepsilon_\tau(\boldsymbol{c}_k) = \frac{\sigma}{\sqrt{2\pi}\|\boldsymbol{c}_k\|} \mathrm{E}\left[ \exp\left( \frac{-(\boldsymbol{c}_k^T\mathbf{H}\tilde{\boldsymbol{x}} - \tau)^2}{2\|\boldsymbol{c}_k\|^2\sigma^2} \right) \right] \tag{33}$$

and

$$q_\tau(\boldsymbol{c}_k) = \mathrm{E}\left[ Q\left( \frac{\boldsymbol{c}_k^T\mathbf{H}\tilde{\boldsymbol{x}} - \tau}{\|\boldsymbol{c}_k\|\sigma} \right) \mathbf{H}\tilde{\boldsymbol{x}} \right]. \tag{34}$$

We see that if the norm of $\boldsymbol{c}_k$ is sufficiently small relative to $\tau$, $\varepsilon_\tau(\boldsymbol{c}_k)$ is effectively zero and (32) becomes $\boldsymbol{c}_{k+1} = \boldsymbol{c}_k + \mu q_\tau(\boldsymbol{c}_k)$. But, as shown in [5], $q_\tau(\boldsymbol{c}_k)$ is a vector with a non-zero lower-bounded norm; hence, the norm of $\boldsymbol{c}$ cannot shrink to zero.

## References


[1] E. Shamash and K. Yao, "On the Structure and Performance of a Linear Decision Feedback Equalizer Based on the Minimum Error Probability Criterion," *International Conference on Communications*, pp. 25F1-25F5, 1974.

[2] P. Galko and S. Pasupathy, "Optimal Linear Receiver Filters for Binary Digital Signals." *International Conference on Communications*, pp. 1H.6.1-1H.6.5, 1982.

[3] S. Chen, E. Chng, B. Mulgrew, and G. Gibson, "Minimum-BER Linear-Combiner DFE," *International Conference on Communications*, pp. 1173-1177, 1996.

[4] C.-C. Yeh and J. R. Barry, "Approximate Minimum-Bit Error Rate Equalization for Binary Signaling," *International Conference on Communications*, pp. 1095-1099, 1997.

[5] C.-C. Yeh and J. R. Barry, "Approximate Minimum-Bit Error Rate Equalization for Binary Signaling," submitted to *IEEE Transactions on Communications*, May 1997.

[6] R. Sharma, W. Sethares, and J. Bucklew, "Asymptotic Analysis of Stochastic Gradient-Based Adaptive Filtering Algorithms with General Cost Functions," *IEEE Transactions on Signal Processing*, pp. 2186-2194, September 1996.

[7] C. P. Kwong, "Dual Sign Algorithm for Adaptive Filtering," *IEEE Transactions on communications*, pp.1272-1275, December 1986.